PHYSICAL REVIEW B **85**, 081303(R) (2012)

Exciton acoustic-phonon coupling in single GaN/AlN quantum dots

Irina A. Ostapenko,* Gerald Hönig, Sven Rodt, Andrei Schliwa, Axel Hoffmann, and Dieter Bimberg
Institut für Festkörperphysik, Technische Universität Berlin, Hardenbergstrasse 36, 10623 Berlin, Germany

Matthias-René Dachner, Marten Richter, and Andreas Knorr
Institut für Theoretische Physik, Technische Universität Berlin, Hardenbergstrasse 36, 10623 Berlin, Germany

Satoshi Kako and Yasuhiko Arakawa
Research Center for Advanced Science and Technology, University of Tokyo, 4-6-1 Komaba, Meguro, Tokyo 153-8904, Japan
(Received 1 November 2011; published 6 February 2012)

Coupling of acoustic phonons to excitons in single wurtzite-type GaN/AlN quantum dots is investigated in detail by cathodoluminescence experiments and compared to theory. Numerical simulations of the coupling in the framework of the independent Boson model with realistic wave functions based on 8-band $\mathbf{k}\cdot\mathbf{p}$ theory show good agreement with observed emission line shapes. We analyze the influence of the geometry and the built-in dipole moment of the quantum dots on the spectral distribution of phonon-coupling strength and the different coupling mechanisms. We observe considerable contribution of the transversal phonons via piezoelectric coupling. The omnipresent broadening of the zero-phonon line is discussed in terms of spectral diffusion.

DOI: 10.1103/PhysRevB.85.081303 PACS number(s): 78.67.Hc, 78.55.Cr, 73.21.La, 63.22.−m

Introduction. Elastic and inelastic interaction of acoustic phonons and charge carriers in quantum dots (QDs) influences the line shape of excitonic single-dot luminescence. The former contributes to the Lorentzian width of the zero-phonon line (ZPL), whereas the inelastic contributions predominantly determine the shape of the phonon sidebands and may also lead to ZPL broadening. Both effects were studied in experimental[1–4] and theoretical works.[5–10]

Although an electron-hole pair is a neutral particle in terms of the associated net charge, the spatial charge distributions of electrons and holes differ, resulting in local lattice distortions. When the exciton decays, the lattice distortion relaxes, leading to the emission of acoustic phonons visible as a low-energy sideband in the luminescence spectrum. An acoustical phonon mode forms alternating areas of compressive and tensile strain changing in time and space, associated with a local variation of the band gap via deformation potential interaction. If the crystal lattice lacks inversion symmetry, there is also interaction via a traveling piezoelectric field.[11] By those two effects the acoustic phonon interacts with the charge carriers inside the QD, possibly leading also to phonon absorption. The carrier-phonon coupling strength mainly depends on a number of parameters: the shape of the excitonic wave function, in particular the associated electric dipole moment and the wave-function extension, the phonon dispersion, and both the deformation potential and piezoelectric constants.

Exciton-phonon interaction in QDs is of interest both for basic research and for the use of single QDs in quantum information schemes.[12,13] In particular, interaction with phonons is known to be a major reason for dephasing and the loss of coherence of excitonic states.[14,15] Furthermore, in the presence of spin-orbit coupling, spin-flip processes between the bright exciton states[16] or from bright into dark states as well as energy-transfer processes between QDs and higher-energy carrier reservoirs[17] can be phonon mediated.

In this Rapid Communication, we measure and model the excitonic line shape of single GaN/AlN QDs. Owing to their deep confinement potential, such QDs are of particular interest for the development of room-temperature single and entangled q-bit emitters for quantum cryptography. Stable single-photon emission from GaN/AlN QDs up to 200 K was observed previously.[18] Acoustic-phonon coupling influences the emission line shape and width and has a large impact on the properties of the aforementioned devices. Insight into QD-phonon coupling is therefore crucial for the application of single QDs. Peculiar to wurtzite-type nitride QDs are the huge built-in piezo- and pyroelectric fields. They result in a separation of the electron and hole wave function, thus creating a significant built-in dipole moment.[19] Since GaN/AlN in the wurtzite phase constitutes a strongly polar material, not only does the deformation potential coupling contribute to the phonon interaction, but also a strong piezoelectric coupling is found to be essential. The latter scales with the size of the built-in dipole moment, as we will show by presenting numerical results for different QD geometries. This dipole makes the confined excitons very sensitive to electric fields in the local environment of the QDs.[20,21] Indeed, inhomogeneous broadening due to spectral diffusion is suggested to cause the large emission linewidths of wurtzite-type GaN/AlN QDs as compared to arsenide QDs[22] or even GaN/AlN QDs grown along nonpolar directions.[23,24]

Experiments and numerical modeling. We study samples of wurtzite-type GaN/AlN QDs grown by low-pressure metal-organic vapor deposition in the Stranski-Krastanow growth mode on (0001)-oriented 6H-SiC substrates. A detailed growth description can be found in Ref. 25. To isolate single QDs, samples are processed using electron beam lithography into mesa structures with a smallest diameter of 200 nm.

The luminescence from single QDs was measured in a scanning electron microscope JEOL JSM 840 equipped with a cathodoluminescence (CL) setup.[26] The acceleration voltage was 3 keV allowing for excitation of the QDs via the AlN matrix. A He-flow cryostat provides temperatures as low as 5 K. Spectra were recorded with a liquid-nitrogen–

cooled Si charge-coupled-device camera. The luminescence was dispersed in a 30-cm monochromator equipped with a 2400 lines mm^{-1} grating, resulting in a spectral resolution of 0.8 meV at 4.2 eV. The shortest integration time for single spectra with sufficient signal-to-noise ratio (SNR) was as short as 50 ms. For a better SNR most spectra shown here were measured with longer integration times (up to 20 s).

The coupling between excitons and acoustic phonons is calculated in the framework of the independent Boson model, which is exactly solvable. Here, the QDs are assumed to be a two-level system that couples to a phonon bath via band diagonal coupling.[11,27–29] The model includes both longitudinal (LA) and transverse acoustic (TA) phonons. The only input parameters are the QD wave functions and the material parameters. Since the interaction between phonons and confined charge carriers occurs within the dot, the deformation potential and piezoelectric constants of GaN are used to obtain realistic results (see also Ref. 11). The phonon dispersion by contrast is described via AlN bulk phonon modes. The intrinsic homogeneous width of the calculated ZPL was chosen to correspond to the radiative decay time of approximately 1 ns.[30] Here, additional contributions to homogeneous broadening, such as nondiagonal coupling to higher states[7,10,31] or a finite phonon lifetime,[3,8,9] are not considered. Also, inhomogeneous broadening due to spectral diffusion[20,24,32,33] is not included. Hence the calculated ZPLs appear in our model with larger intensity and smaller width than in the experiments. However, we demonstrate below that calculated and experimentally obtained amplitudes match very well when spectral diffusion is superimposed.

Characteristic for electronic states in *c*-plane GaN/AlN QDs is their strong vertical electron-hole separation resulting from the large piezo- and pyroelectric fields.[34] For an adequate description of the confined carriers, realistic wave functions from 8-band $\mathbf{k}\cdot\mathbf{p}$ theory are used as a starting point for calculating the exciton-phonon coupling. Direct Coulomb and exchange effects are considered by self-consistently solving the Hartree-Fock equations.[35]

The benefit of using 8-band $\mathbf{k}\cdot\mathbf{p}$ functions was already shown in our previous work.[4] Analytical wave functions of Gaussian type failed to describe the interaction with phonons having larger wave numbers, as well as they failed to yield similar sideband shapes; hence, there is no quantitative agreement with our experimental results.

Results and discussion. Emission lines from single QDs show pronounced asymmetric sidebands on the low-energy side, even at temperatures as low as 5 K (Fig. 1). The change of the line shape with temperature of one typical line is shown on a relative energy scale. The change of the energetic position of the peak maximum is shown in the inset in Fig. 1. All spectra are normalized relative to their integrated intensity to emphasize the distribution of emitted photons among the ZPL and the sideband. With increasing temperature the low-energy sideband gains in intensity with respect to the central peak, and a high-energy sideband emerges. The central line shape deviates strongly from either Lorentzian or Gaussian types. The sidebands can neither be assigned to background luminescence, often observed for nitride-based QDs,[20,36] nor ascribed to luminescence features from another QD. Indeed, the time evolution of the sidebands shows the same spectral

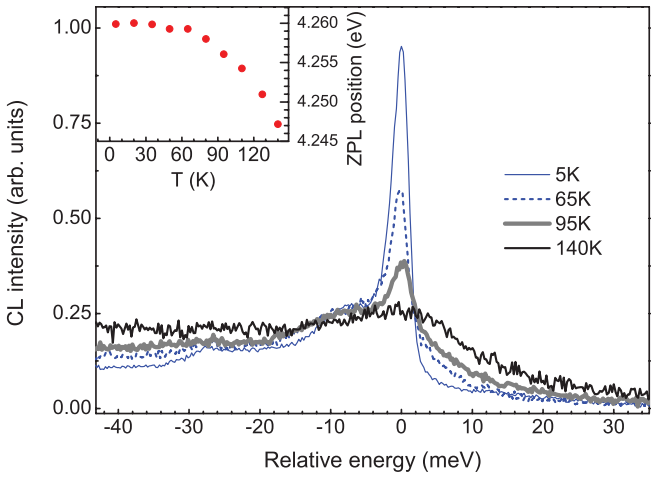

FIG. 1. (Color online) Temperature dependence of a single emission line with respect to the ZPL. Inset: Temperature dependence of the energetic position of the ZPL.

diffusion pattern as the central peak, confirming the same local origin.[20,32,33]

Such line shapes are typical for inelastic scattering of acoustic phonons with charge carriers in QDs.[1] The central emission line, which we identify as the ZPL, results from a radiative recombination process in the QD without energy loss/gain due to phonon emission or absorption. This ZPL is surrounded by a continuum of phonon-assisted radiative transitions. Phonon emission and absorption rates for a given phonon mode are proportional to $\boldsymbol{(}n(\omega,T)+1\boldsymbol{)}$ and $n(\omega,T)$, respectively, where $n(\omega,T)$ is the phonon occupation number as given by the Bose-Einstein distribution for temperature T and phonon frequency ω. Both processes contribute to the low-energy (emission) and high-energy (absorption) sidebands of the ZPL. Since $n(\omega,T)$ is small for low temperatures, only phonon emission occurs, resulting in highly asymmetric line shapes. At higher temperatures, as $n(\omega,T)$ increases, the probability for phonon emission and absorption converges, resulting in more symmetrical sidebands with increasing T.

Numerical results for the temperature dependence of the spectra are shown in Fig. 2(a). All spectra are normalized relative to their integrated intensity. The evolution of the phonon sidebands as observed in the experiment (Fig. 1) is very well reproduced by the calculated spectra. As noted before, the calculated ZPL is solely represented by a Lorentzian function with a width of 5 μeV, which corresponds to the carrier lifetimes from time-resolved experiments.[30] This way, the ratio of the amplitudes of the phonon sidebands and ZPL is smaller than found in experiment. We attribute this difference to spectral diffusion, which broadens the measured spectra. Spectral diffusion results in smearing the spectral features within the exposure time (the detector sums up spectra at slightly different energetic positions). To verify this effect a calculated spectrum was convoluted with a Voigt profile [the resulting curve is depicted in Fig. 2(b) as solid line]. The width (1.7 meV) of the Voigt profile was fitted to the experimentally observed ZPL [dotted line in Fig. 2(b)] to get the energetic distribution function resulting from spectral

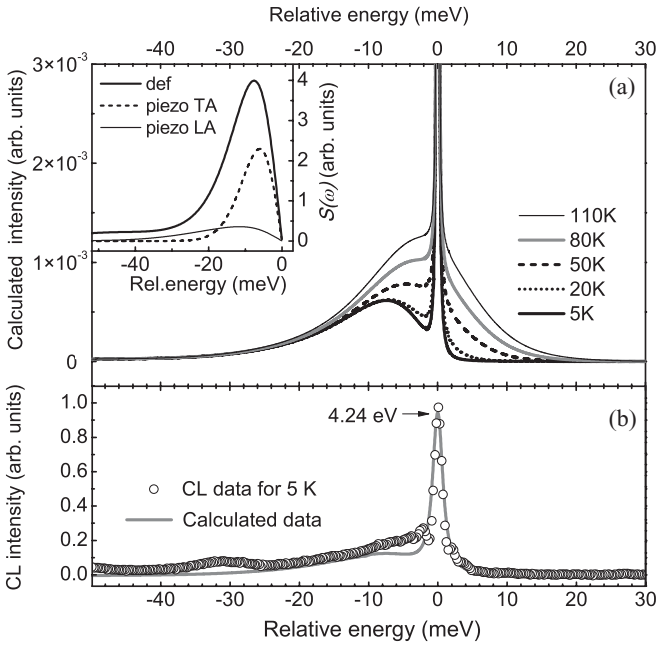

FIG. 2. (a) Calculated temperature dependence of a single emission line. The ZPL peak intensity for the 5 K curve is 1, not shown completely in the figure. The inset shows spectral densities $S(\omega)$ for a model QD with a height of 1.4 nm, base length of 7 nm, and emission energy of 4.03 eV. (b) Comparison of experimental data (dotted line, CL measured at 5 K, ZPL energy at 4.24 eV) and calculated spectrum (solid line), with the latter including the effect of spectral diffusion as described in the text.

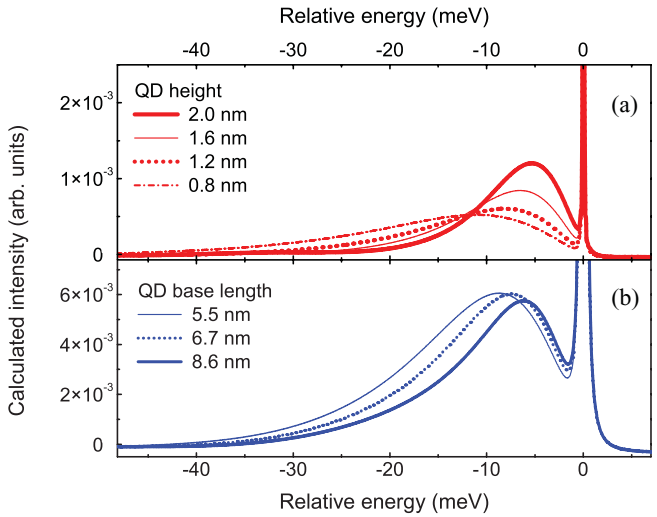

FIG. 3. (Color online) (a) Calculated spectra for model QDs with the same aspect ratio of 0.2 and different height (i.e., electron-hole separation). The height (base length) increases from 0.8 nm (4 nm) up to 2.0 nm (10 nm). The QD emission energy decreases from 4.8 to 3.6 eV. (b) Calculated spectra of model QDs with the same height of 1.2 nm and varying base length from 5.5 to 8.6 nm. The QD emission energy changes from 4.3 to 4.1 eV. In both graphs the ZPL intensity is 1, not shown completely.

diffusion. Both spectra are plotted in Fig. 2(b) and now exhibit a good agreement of ZPL and phonon sideband amplitudes.

The observed phonon sidebands are unusually strong as compared to other material systems, such as InGaAs/GaAs QDs (e.g., Ref. 4), presenting an obstacle for utilizing GaN/AlN QDs in quantum communication. Thus, it is important to investigate the origin of the strong coupling and its dependence on the structural properties of the QDs for better understanding and control of the interaction. For that purpose we separate the impact of deformation-potential coupling and piezoelectric coupling. The former is effective for LA phonons only, whereas the latter includes both LA and TA phonons.

The inset of Fig. 2(a) shows the spectral densities $S(\omega)$ of phonon-coupling mechanisms for our model QD, corresponding to the low-energy sideband at 0 K. Here, $S(\omega) = \sum_{\vec{q}} \frac{|g^{\vec{q}\kappa}|^2}{\hbar^2\omega^2}\delta(\omega - \omega_\kappa(\vec{q}))$, where $g^{\vec{q}\kappa}$ is the coupling element of the exciton to a phonon in mode κ with wave vector $\vec{q}$, calculated from the carrier wave functions, and $\omega_\kappa(\vec{q})$ is the phonon frequency. The piezoelectric coupling plays an important role in nitride-based materials[11,29] and cannot be neglected as in arsenides.[4,5] At small energies (wave vectors) the contribution of piezoelectric coupling to TA phonons is larger than piezoelectric coupling to LA phonons and of the same order of magnitude as deformation-potential coupling. Furthermore, the combined $S(\omega)$ has a maximum for a relative energy of 10 meV, which is in the range of fine-structure splitting for these QDs.[35] Consequently, in the presence of spin-orbit coupling, spin-flip processes between the bright-exciton states may be also promoted by the interaction with acoustic phonons.[16]

Next we will analyze the dependence of phonon coupling on the structural parameters of the QDs. Figure 3(a) shows numerical results for QDs of different geometry where we kept the aspect ratio constant at 0.2 (ratio of height to base length) and varied the height of the QD from 0.8 to 2 nm (i.e., base length from 4 to 10 nm). This size variation refers to experimental observations of the size evolution of self-organized GaN/AlN QDs.[18,25,35] The results show that the height of the low-energy phonon shoulder increases monotonously with QD size. We associate this trend with a strong influence of the built-in piezo- and pyroelectric fields. The higher the dot becomes, the larger the drop of the built-in potentials within the QD, leading to an increase of the excitonic electron-hole dipole moment with increasing QD height. Consequently, the larger the permanent dipole moment, the larger the coupling to acoustic phonons via piezoelectric coupling. These findings correspond well to our experimental observations: For small emission energies hardly any distinct lines could be resolved, although the spectral resolution of the setup is better in this spectral range. In addition, taller QDs are more sensitive to their environment and show enhanced spectral diffusion. Thus for larger dots their larger phonon sidebands [as shown in Fig. 3(a)] can become as intense as the broadened ZPL.

Model calculations for QDs of the same height (1.2 nm) but of different lateral sizes (variation from 5.5 up to 8.6 nm) show almost no influence of the QD base length on the height of the phonon shoulder [Fig. 3(b)]; only the maximum of the phonon shoulder shifts toward the ZPL with increasing base length.

Detailed analysis of the spectral density for deformation-potential coupling $S(\omega)_{\text{def}}$ and piezoelectric coupling $S(\omega)_{\text{piezo}}$ allows for the same general statements: The amplitude of $S(\omega)_{\text{def}}$ goes down when the extension of the wave functions increases, but does not depend on the excitonic permanent dipole moment. The amplitude of $S(\omega)_{\text{piezo}}$, in contrast, is almost independent of the lateral extent of the wave function but increases monotonously with increasing permanent dipole moment. Both $S(\omega)_{\text{def}}$ and $S(\omega)_{\text{piezo}}$ get closer to the ZPL for increasing wave-function extent regardless of the permanent dipole moment.

Conclusion. Strong acoustic-phonon coupling in single GaN/AlN QDs is observed in temperature-dependent cathodoluminescence experiments. The carrier-phonon interaction is calculated in the framework of the independent Boson model using realistic electron and hole wave functions calculated from 8-band $\mathbf{k} \cdot \mathbf{p}$ theory. Our model accounts very well for the experimental observations of the shape and position of the phonon sidebands. Piezoelectric coupling is found to be of the same order of magnitude as deformation potential coupling. The interaction with transverse acoustic phonons is found to be of large importance. The analysis of QDs with different permanent dipole moments shows enhanced phonon sidebands for larger dipole moments, i.e., taller QDs.

Acknowledgments. This work was supported by Deutsche Forschungsgemeinschaft in the framework of SFB 787 and the Creation of Innovation Centers for Advanced Interdisciplinary Research Areas Program, MEXT Japan. We thank David Gershoni, Ulrike Woggon, Christian H. Kindel, and Volker Türck for fruitful discussions.

*irina@sol.physik.tu-berlin.de

[1] L. Besombes, K. Kheng, L. Marsal, and H. Mariette, Phys. Rev. B **63**, 155307 (2001).

[2] P. Borri, W. Langbein, S. Schneider, U. Woggon, R. L. Sellin, D. Ouyang, and D. Bimberg, Phys. Rev. Lett. **87**, 157401 (2001).

[3] G. Ortner, D. R. Yakovlev, M. Bayer, S. Rudin, T. L. Reinecke, S. Fafard, Z. Wasilewski, and A. Forchel, Phys. Rev. B **70**, 201301 (2004).

[4] E. Stock, M.-R. Dachner, T. Warming, A. Schliwa, A. Lochmann, A. Hoffmann, A. I. Toropov, A. K. Bakarov, I. A. Derebezov, M. Richter, V. A. Haisler, A. Knorr, and D. Bimberg, Phys. Rev. B **83**, 041304 (2011).

[5] B. Krummheuer, V. M. Axt, and T. Kuhn, Phys. Rev. B **65**, 195313 (2002).

[6] J. Förstner, K. Ahn, J. Danckwerts, M. Schaarschmidt, I. Waldmüller, C. Weber, and A. Knorr, Phys. Status Solidi B **234**, 155 (2002).

[7] E. A. Muljarov, T. Takagahara, and R. Zimmermann, Phys. Rev. Lett. **95**, 177405 (2005).

[8] B. Krummheuer, V. M. Axt, and T. Kuhn, Phys. Rev. B **72**, 245336 (2005).

[9] P. Machnikowski and L. Jacak, Phys. Rev. B **71**, 115309 (2005).

[10] T. Grange, Phys. Rev. B **80**, 245310 (2009).

[11] B. Krummheuer, V. M. Axt, T. Kuhn, I. D'Amico, and F. Rossi, Phys. Rev. B **71**, 235329 (2005).

[12] A. Lochmann, E. Stock, J. A. Tofflinger, W. Unrau, A. Toropov, A. Bakarov, V. Haisler, and D. Bimberg, Electron. Lett. **45**, 566 (2009).

[13] C. L. Salter, R. M. Stevenson, I. Farrer, C. A. Nicoll, D. A. Ritchie, and A. J. Shields, Nature **465**, 594 (2010).

[14] U. Hohenester, G. Pfanner, and M. Seliger, Phys. Rev. Lett. **99**, 047402 (2007).

[15] A. Carmele, F. Milde, M.-R. Dachner, M. B. Harouni, R. Roknizadeh, M. Richter, and A. Knorr, Phys. Rev. B **81**, 195319 (2010).

[16] L. M. Woods, T. L. Reinecke, and Y. Lyanda-Geller, Phys. Rev. B **66**, 161318 (2002).

[17] M.-R. Dachner, E. Malic, M. Richter, A. Carmele, J. Kabuss, A. Wilms, J.-E. Kim, G. Hartmann, J. Wolters, U. Bandelow, and A. Knorr, Phys. Status Solidi B **247**, 809 (2010).

[18] S. Kako, C. Santori, K. Hoshino, S. Gotzinger, Y. Yamamoto, and Y. Arakawa, Nat. Mater. **5**, 887 (2006)

[19] T. Bretagnon, S. Kalliakos, P. Lefebvre, P. Valvin, B. Gil, N. Grandjean, A. Dussaigne, B. Damilano, and J. Massies, Phys. Rev. B **68**, 205301 (2003).

[20] R. Bardoux, T. Guillet, P. Lefebvre, T. Taliercio, T. Bretagnon, S. Rousset, B. Gil, and F. Semond, Phys. Rev. B **74**, 195319 (2006).

[21] I. A. Ostapenko, G. Hönig, C. Kindel, S. Rodt, A. Strittmatter, A. Hoffmann, and D. Bimberg, Appl. Phys. Lett. **97**, 3 (2010).

[22] M. Bayer and A. Forchel, Phys. Rev. B **65**, 041308 (2002).

[23] J. P. Garayt, J. M. Gérard, F. Enjalbert, L. Ferlazzo, S. Founta, E. Martinez-Guerrero, F. Rol, D. Araujo, R. Cox, B. Daudin, B. Gayral, L. Si Dang, and H. Mariette, Physica E **26**, 203 (2005).

[24] F. Rol, S. Founta, H. Mariette, B. Daudin, L. S. Dang, J. Bleuse, D. Peyrade, J.-M. Gérard, and B. Gayral, Phys. Rev. B **75**, 125306 (2007).

[25] K. Hoshino, S. Kako, and Y. Arakawa, Appl. Phys. Lett. **85**, 1262 (2004).

[26] J. Christen, M. Grundmann, and D. Bimberg, J. Vac. Sci. Technol. B **9**, 2358 (1991).

[27] R. Zimmermann and E. Runge, in *Proceedings 26th ICPS Edinburgh*, IOP Conf. Series, Vol. 171, edited by A. R. Long and J. H. Davies (IOP, Bristol, 2002).

[28] J. Förstner, C. Weber, J. Danckwerts, and A. Knorr, Phys. Status Solidi B **238**, 419 (2003).

[29] A. Vagov, M. D. Croitoru, V. M. Axt, P. Machnikowski, and T. Kuhn, Phys. Status Solidi B **248**, 839 (2011).

[30] S. Kako, M. Miyamura, K. Tachibana, K. Hoshino, and Y. Arakawa, Appl. Phys. Lett. **83**, 984 (2003).

[31] E. A. Muljarov and R. Zimmermann, Phys. Rev. Lett. **98**, 187401 (2007).

[32] V. Turck, S. Rodt, O. Stier, R. Heitz, R. Engelhardt, U. W. Pohl, D. Bimberg, and R. Steingruber, Phys. Rev. B **61**, 9944 (2000).

[33] J. H. Rice, J. W. Robinson, A. Jarjour, R. A. Taylor, R. A. Oliver, G. A. D. Briggs, M. J. Kappers, and C. J. Humphreys, Appl. Phys. Lett. **84**, 4110 (2004).

[34] M. Winkelnkemper, R. Seguin, S. Rodt, A. Hoffmann, and D. Bimberg, J. Phys. Condens. Matter **20**, 454211 (2008).

[35] C. Kindel, S. Kako, T. Kawano, H. Oishi, Y. Arakawa, G. Hönig, M. Winkelnkemper, A. Schliwa, A. Hoffmann, and D. Bimberg, Phys. Rev. B **81**, 241309 (2010).

[36] D. Simeonov, A. Dussaigne, R. Butte, and N. Grandjean, Phys. Rev. B **77**, 5 (2008).